

ARTICLES

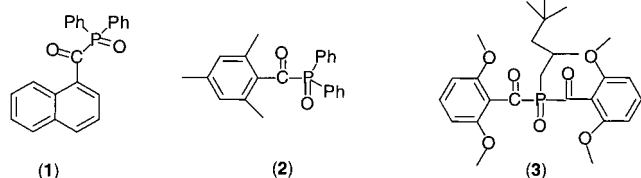
Photochemistry and Photophysics of (1-Naphthoyl)diphenylphosphine Oxide

Ningning Zhao, Bernd Strehmel, Anthony A. Gorman,[†] Ian Hamblett,[†] and Douglas C. Neckers^{*,‡}*Center for Photochemical Sciences,¹ Bowling Green State University, Bowling Green, Ohio 43403, and Chemistry Department, University of Manchester, Manchester, M13 9PL, U.K.**Received: April 2, 1999; In Final Form: June 11, 1999*

(1-Naphthoyl)diphenylphosphine oxide (**1**) was synthesized and characterized and its photochemistry investigated using emission spectroscopy, pulse radiolysis, and nanosecond laser flash photolysis. Fluorescence quantum yields are low in aprotic polar and nonpolar solvents. In methanol, as a result of hydrogen-bonding, change of S_1 from an n,π^* state to a π,π^* state leads to the decrease in the rate constant for intersystem crossing and results, finally, in an increase in fluorescence. Preferential solvation was evaluated using the E_T indicator "Reichardt's dye" (RD). E_T^N values were determined by gradually increasing the concentrations of methanol in methanol/acetonitrile mixtures. Fluorescence quantum yields correlate with the E_T^N values. Photolysis of **1** yields diphenyl[1-naphthoyl]oxy]phosphine (**6**), formed mainly via cage recombination of radicals. No radicals were detected by either nanosecond laser flash photolysis or pulse radiolysis of **1** in aprotic solvents. However, photolysis in methanol yields radicals when **1** is excited at 266 nm. The phosphinoyl radical can be quenched by either methyl methacrylate (MMA) or oxygen ($k_q = 5.0 \times 10^7$ and 5.3×10^8 $M^{-1} s^{-1}$, respectively). Such radical generation most likely results from the singlet excited state.

Introduction

In the past few years, acyl and bis(acyl)phosphine oxides have become important UV photoinitiators for the free-radical polymerization of acrylates.^{2–16} Both aryl acyl and bis(acyl)phosphine oxides undergo rapid α -cleavage from the triplet excited state producing both carbon- and phosphorus-centered radicals.^{5,11c,12,14,15} The radical species formed^{5–16} have been detected by laser flash photolysis using both infrared and UV detection,^{5,13,16} time-resolved ESR,¹¹ CIDNP,¹² and picosecond pump-probe spectroscopy.¹⁵ Thus 2,4,6-trimethylbenzoyl-diphenylphosphine oxide (**2**)^{5,12–14} and bis(2,6-dimethoxybenzoyl)-2,4,4-trimethylpentylphosphine oxide (**3**)^{12,14} are shown to generate both carbon- and phosphorus-centered radicals by α -cleavage of the triplet excited state.



Global analysis has become a standard technique for the examination of fluorescence in biological systems¹⁷ but not for the evaluation of flash photolysis data. We have used this to

obtain more accurate values for the kinetic behavior of the triplet state of **1**. Fluorescence and phosphorescence experiments have considered the emission properties of the excited states of **1** as well.

In this paper, we report the first example of an acyl phosphine oxide, **1**, that undergoes an efficient disappearance but yields no radicals that can be detected either by laser flash photolysis or pulse radiolysis. Compound **1** behaves differently from the analogous phenyl derivatives^{2–16} which are known to efficiently produce radicals. The triplet state is formed in benzene on transient laser excitation as confirmed by pulse radiolysis experiments. Rate constants for the reactions of the diphenylphosphinoyl (**4**) and naphthoyl radical (**5**) with methyl methacrylate (MMA) and O_2 have been determined. Photoproducts obtained after irradiation of **1** have been isolated.

Results and Discussion

Fluorescence and Phosphorescence. The fluorescence quantum yield (ϕ_f) of **1** strongly depends on the nature of the solvent (Table 1). The emission spectra of **1** observed in polar solvents, for example, acetonitrile and methanol (Figure 1), clearly demonstrate that fluorescence is much more intense in a hydrogen-bonding solvent than in non-hydrogen-bonding solvents.

Rate constants for intersystem crossing (k_{isc}) in non-hydrogen-bonding solvents, estimated according to eqs 1 and 2, indicate an efficient transition from singlet to triplet state occurs because of the relatively low values of k_f^0 in aprotic solvents (Table 1).^{18,19}

[†] University of Manchester.[‡] E-mail: neckers@photo.bgsu.edu.

TABLE 1: Photophysical Properties of 1 in Different Solvents

	cyclohexane	benzene	acetonitrile	methanol
ϕ_f^a	4.2×10^{-3}	9.4×10^{-3}	8.1×10^{-4}	0.21
$\epsilon_{\max}(\text{n},\pi^*) (\text{M}^{-1} \text{cm}^{-1})$	451	389	532	
$k_f^0 (\text{s}^{-1})^b$	4.5×10^6	3.9×10^6	5.3×10^6	$\sim 10^{7f}$
$k_{\text{isc}} (\text{s}^{-1})^c$	1.0×10^9	4.0×10^8	6.3×10^9	$\sim 10^{8f}$
$\tau_p (\text{ms})^d$	83			
ϕ_p^e	0.033			
$E_s (\text{kcal/mol})$	64.2	64.2	64.2	87

^a ϕ_f , fluorescence quantum yields in different solvents (fluorescence standard^{22,23} 9,10-diphenylanthracene $\phi_f = 0.95$ (CH₃CN), $\phi_f = 0.90$ (cyclohexane)). ^b k_f^0 , estimated from absorption spectra $10^4 \epsilon_{\max}(\text{n},\pi^*)$. ^c k_{isc} : intersystem crossing rate constant calculated by the relation $k_{\text{isc}} = \phi_T k_f^0 / \phi_f$. ^d Phosphorescence decay time in EPA (ether:isopentane:ethanol = 5:5:2) at 77 K. ^e Phosphorescence quantum yield in EPA (standard:²⁴ benzophenone in EPA $\phi_p = 0.74 \pm 0.02$). ^f This number is an estimate and was calculated from $\tau_s \sim 8$ ns in methanol solution of **1** at 266 nm excitation by nanosecond flash photolysis.

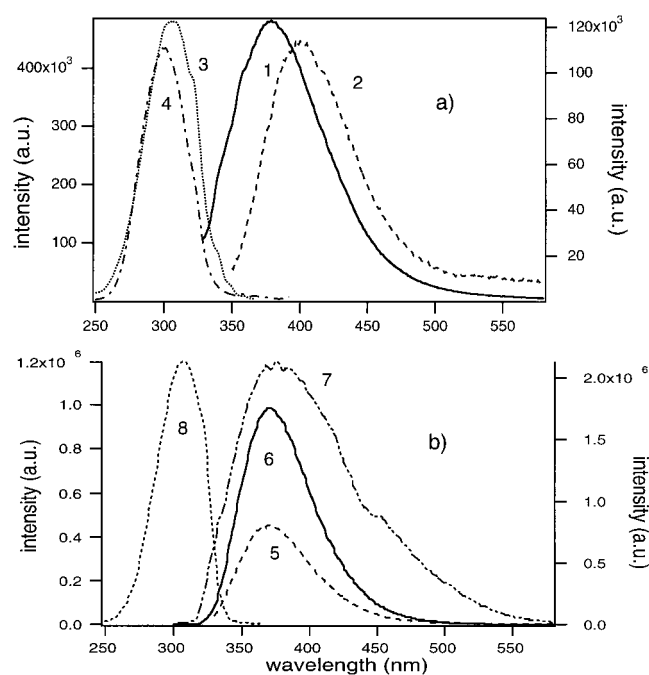


Figure 1. (a) Fluorescence emission (1 and 2) and excitation (3 and 4) spectra of **1** in acetonitrile (1.1×10^{-5} M) at room temperature (1; $\lambda_{\text{ex}} = 322$ nm; 2, $\lambda_{\text{ex}} = 338$ nm; 3, $\lambda_{\text{em}} = 379$ nm; 4, $\lambda_{\text{em}} = 400$ nm) and (b) Fluorescence emission (5 and 6), delayed fluorescence (7) and excitation spectra of **1** (8) in methanol (1.4×10^{-5} M) at room temperature (5, $\lambda_{\text{ex}} = 325$ nm; 6, $\lambda_{\text{ex}} = 296$ nm; 7, after 1 μs delay, $\lambda_{\text{ex}} = 296$ nm; 8, $\lambda_{\text{em}} = 372$ nm). Left axis top: 3 and 4; right top: 1 and 2; left bottom: 8; right bottom: 5, 6, and 7; the intensity for delayed fluorescence, 7, is multiplied by a factor of 450.

$$k_f^0 = \epsilon_{\max} \nu_{\max}^2 \nu_{1/2} \cong 10^4 \epsilon_{\max} \quad (1)$$

ϵ_{\max} is the molar absorption coefficient of n,π^* , ν_{\max} maximum of absorption energy, and $\nu_{1/2}$ half-width of the absorption band.

$$k_{\text{isc}} = \phi_T (k_f^0 / \phi_f) \quad (2)$$

ϕ_T is obtained from laser flash photolysis; (see Table 2), and in aprotic solvents that ϕ_T are assumed the same).

In hydrogen-bonding solvents such as methanol, an increase of k_f^0 and a decrease of k_{isc} is observed. This can be understood if one considers a change of singlet excited states in different solvents with the nature and population of the lowest singlet

TABLE 2: Nanosecond Laser Photolysis Data of 1

	benzene	acetonitrile	methanol
$\tau_T (\mu\text{s})^a$	22	18	25
$k_q (\text{O}_2) \text{M}^{-1} \text{s}^{-1}^a$	1.2×10^9	1.3×10^9	2.2×10^9
$\epsilon_T (\text{L mol}^{-1} \text{cm}^{-1})^b$	5180		
ϕ_T^b	0.97 ± 0.1		
$E_T (\text{kcal/mol})^b$	54.8 ± 0.1		

^a τ_T , triplet decay time in solvents at room temperature obtained from laser flash photolysis and fitted by global analysis. ^b ϵ_T , extinction coefficients of triplet-triplet absorption by sensitized pulse radiolysis. ϕ_T , benzophenone in benzene as a standard. E_T , lowest triplet energy determined from triplet-triplet energy transfer equilibrium with chrysenes.

state resulting in different values. We also observed an increase of 23 kcal/mol in singlet excited-state energy from switching from an aprotic medium (64 kcal/mol) to a protic one (87 kcal/mol).

Thus, the rate constants for fluorescence, k_f^0 , indicate it to be dependent on surroundings.¹⁹ A further explanation is based on excited state configuration. Since the change of the solvent from an aprotic to a protic one results in a change of the nature in the excited state, we would expect different transitions.²⁰ In non-hydrogen-bonding solvents, efficient spin-orbit coupling between $^1(\text{n},\pi^*)$ and $^3(\pi,\pi^*)$ states results in rapid intersystem crossing. In contrast, inefficient intersystem crossing occurs between $^1(\pi,\pi^*)$ and $^3(\pi,\pi^*)$ in protic solvents. Therefore, fluorescence competes with the reduced efficiency for intersystem crossing, which leads finally to an increase in ϕ_f . Similar effects were previously reported for naphthaldehydes.²¹

Groups attached to the C-P single bond in **1** can freely rotate. As a result, at least two ground state conformations, for example S-cis and S-trans, may exist in equilibrium at room temperature because there is a low energy barrier. In the excited state of **1** this bond property may change from single bond to double bond in a manner similarly reported for polyenes. Since rotation about a double bond requires a higher activation energy than rotation about a single bond, the energy barrier to interconversion of the conformers by single bond rotation becomes higher in their respective excited states, and an equilibrium process forming the isomers of **1** becomes impossible. Therefore, different conformers of the ground state can be excited to different singlet excited states and the latter are not interconvertible.

Excitation at different wavelengths into the mixed n,π^* and π,π^* band in aprotic polar solvents (i.e., acetonitrile) clearly provides evidence for two different emission spectra (e.g. curves 1 and 2 in Figure 1), caused by depopulation of two different excited singlet states. In contrast, changing the solvent to methanol results, as reported above, in an increase of the energy of excited singlet state and therefore, presumably, to the excitation of one species.

The n,π^* band in the absorption spectrum of **1** can easily be distinguished from the π,π^* band, Figure 2. In aprotic solvents such as cyclohexane, benzene, and acetonitrile, one observes a band of low intensity as a long tail around 400 nm that shifts to the blue as the solvent polarity increases. In methanol, this band disappears likely because of the hydrogen bonding that leads to a further blue shift.²⁵

Compound **1** exhibits phosphorescence emission with vibrational fine structure in EPA (ether:isopentane:ethanol = 5:5:2) glass at 77 K upon excitation at 423 nm (Figure 3). The difference between the (0,0) and (0,1) emission bands is 1456 cm^{-1} , corresponding approximately to a stretching mode in the IR spectrum. The (0,0) emission band at 528 nm corresponds

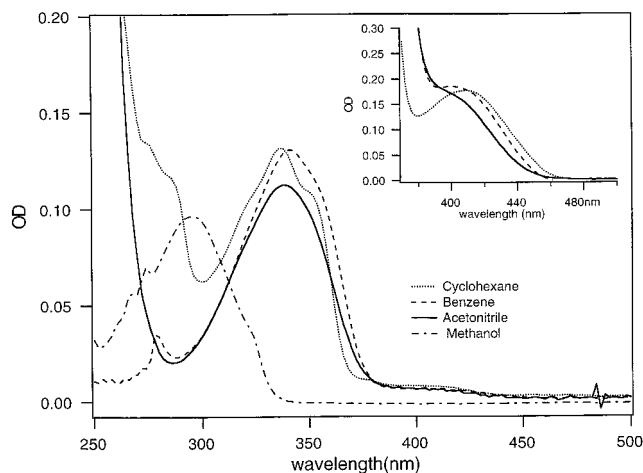


Figure 2. Ground state absorption spectra of **1** in different solvents (1.0×10^{-4} M) Inset: ground state absorption spectra magnified around 400 nm in cyclohexane, benzene, and acetonitrile 1.0×10^{-3} M).

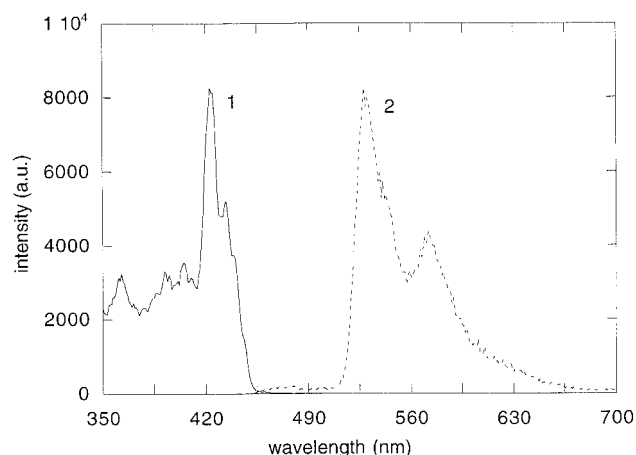
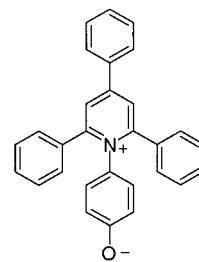


Figure 3. Normalized phosphorescence of **1**; excitation (1) $\lambda_{em} = 529$ nm and emission (2) at $\lambda_{ex} = 423$ nm spectra in EPA (ether:isopentane:ethanol = 5:5:2 in volume) at 77 K.

to a triplet energy 54.2 kcal/mol. The phosphorescence decay time is 83 ms in EPA glass, which is in the range for compounds possessing a lowest $^3(\pi, \pi)^*$ triplet excited state. It is well accepted that the singlet–triplet splitting, ΔE_{ST} , of the n, π^* state is smaller than that of π, π^* states. The experimental value ΔE_{ST} for **1** is around 10 kcal/mol because of n, π nature of lowest singlet excited state.¹⁸

With the gradual addition of methanol to a solution of **1** in acetonitrile the intensity of the absorption at 338 nm decreases while that of the absorption at 296 nm increases. This indicates that the nature of the singlet excited state changes gradually from the non-hydrogen-bonding solvent to the hydrogen-bonding solvent. Thus, the presence of the hydrogen-bonding solvent, methanol, causes an increase in π, π^* contribution in S_1 , and also increases ϕ_f by a factor of approximately 10^2 – 10^3 . From plots of ϕ_f vs [MeOH], a critical point is observed when the excitation is carried out either at 296 nm or at 338 nm, Figure 4. Beyond this critical point, the fluorescence quantum yields level off. Two lines with different slopes are obtained, and these have an intersection point at about 5 wt % methanol.

A more detailed understanding of such solvent effects is obtained using the solvent indicator Reichardt's dye (RD)²⁶ to evaluate the solvent polarity parameter E_T^N in the mixtures of acetonitrile/methanol.



RD

E_T^N values²⁷ were measured in mixtures of acetonitrile/methanol, Figure 5. The relationship between the E_T^N values and the molar fraction of solvent x_2 is given by eq 3, where E_T^{N1} and E_T^{N2} are the E_T^N values of the pure solvent and the index 1 refers to acetonitrile and the index 2 to methanol. The ratio f_2/f_1 is equal to the preferential solvation coefficient and indicates the preferred solvation of the solute RD in the mixture. This ratio further reports which solute possesses the better solubility in each respective solvent. When this value approaches unity, there is no preferred solvation; the solute is equally soluble in either solvent.

$$E_T^N = \frac{E_T^{N1} + x_2 \left(\frac{f_2}{f_1} E_T^{N2} - E_T^{N1} \right)}{1 + x_2 \left(\frac{f_2}{f_1} - 1 \right)} \quad (3)$$

Using Marquardt's nonlinear fit procedure²⁸ there is 13.4 times relative preferential solvation for RD in methanol in comparison to acetonitrile (Figure 5). Furthermore, a satisfactory correlation was found between the fluorescence quantum yields of **1** measured in mixtures of methanol and acetonitrile, and the solvent polarity parameter E_T^N (inset Figure 5). The E_T^N values contain all parameters, including the effect of hydrogen bonding, that describe the solvation of solutes on a microscopic scale. Therefore, a linear change of this parameter leads to a change of the quantity ϕ_f . Excitation at either 338 or 296 nm yields similar results. We conclude, therefore, that **1** is preferentially solvated by methanol rather than by acetonitrile. After saturation, the quantum yield increases more slowly, Figure 4.

Nanosecond Laser Flash Photolysis. Laser flash photolysis of **1** (excitation 355 nm) shows similar transient absorption spectra between 280 nm–700 nm both in benzene and in $\text{CH}_3\text{-CN}$ (Figure 6). The peak from 350 nm to shorter wavelengths evidences bleaching where **1** possesses strong ground state absorption. Surprisingly, the transient species between 370 and 700 nm with maximum absorptions at 380 and 580 nm decay on a microsecond time scale with rather different kinetics. At low laser power, the transient species at 580 nm decays monoexponentially. We attribute this transient to the triplet of **1**. Decays at the different wavelengths were fitted by global analysis²⁹ with monoexponential kinetics. Transient absorption spectra (26 time profiles between 450 and 700 nm) were linked to one data set where only the preexponential factors were a function of the registration wavelength and the calculated decay times were equal for each wavelength. Figure 6 shows a representative decay for **1** in benzene at a registration wavelength of 580 nm. In general, the change in optical density at each wavelength can be described by eq 4, though decay times are almost the same at each wavelength.

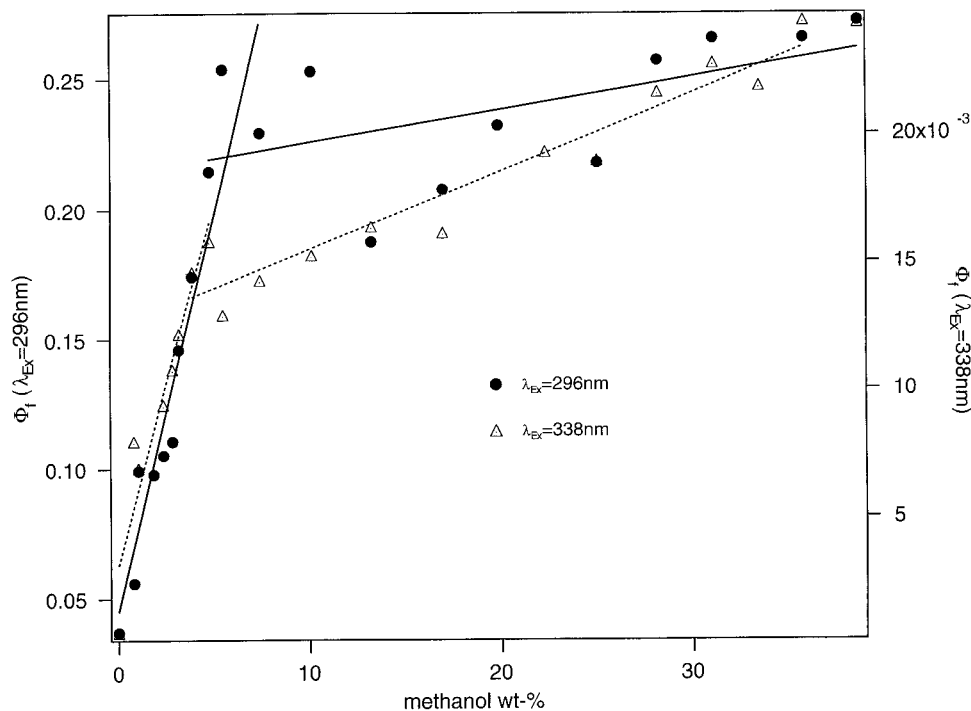


Figure 4. Relationship of fluorescence quantum yield in acetonitrile/methanol mixture vs methanol wt %.

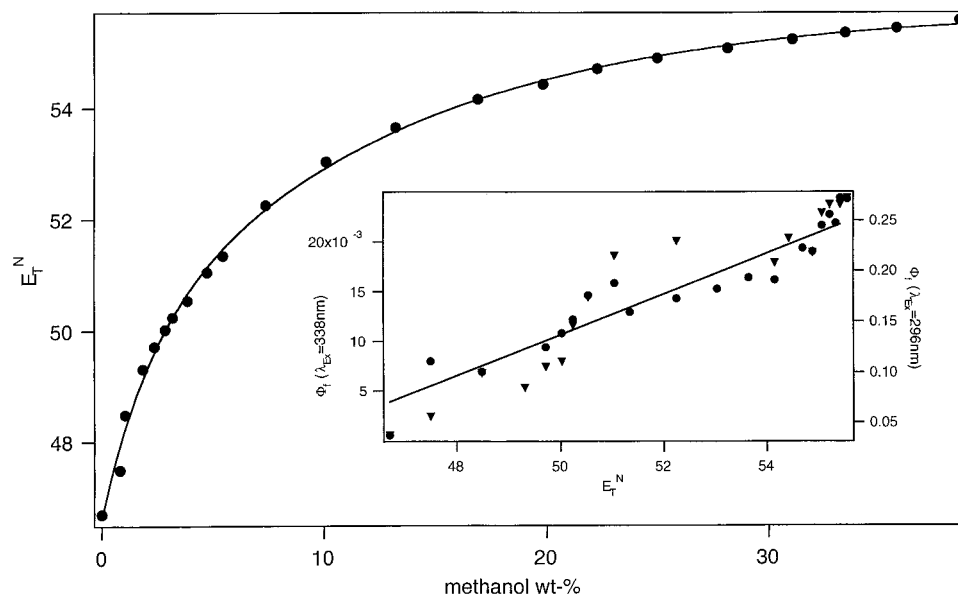


Figure 5. Nonlinear relationship of E_T^N values of Reichardt's dye vs methanol (wt %) acetonitrile/methanol binary system with preferential solvation. Inset: The relationship of fluorescence quantum yield in acetonitrile/methanol mixture solvent with E_T^N (∇ , $\lambda_{\text{ex}} = 338$ nm; \bullet , $\lambda_{\text{ex}} = 296$ nm).

$$\Delta\text{OD}(t, \lambda_i) = \text{BG}(\lambda_i) + \sum_{i=1}^n \alpha_i(\lambda_i) \exp(-4.5 \times 10^4 t) \quad (4)$$

where BG = background, α are preexponential factors.

Evidence for formation of the triplet states of **1** in benzene and acetonitrile was obtained from O_2 quenching experiments, sensitized pulse radiolysis, and from triplet-triplet energy transfer experiments. Sensitized pulse radiolysis showed that the triplet absorption covered the region from 370 to 700 nm. No radical species were detected since none of the decay curves behaved according to a second-order kinetic law.³⁰ The triplet is quenched by oxygen, yielding bimolecular quenching constants that are on the order of one-ninth diffusion control. The data obtained are compiled in Table 2.

The species at 380 nm decays much more slowly than does

the triplet state. There is a long-lived species in that region fitted by a combination of first- and second-order kinetics because of the overlap of the triplet absorption and that of the naphthoyl radical. The naphthoyl radical is present in small amounts and is likely generated from the singlet excited state.

The addition of either methyl methacrylate (MMA) or oxygen reduced the decay time of the naphthoyl radical and results in pseudo-first-order decay kinetics. Bimolecular quenching constants (k_q) for the naphthoyl radical were obtained from plots of the pseudo-first-order rate constants for the decay of transient absorption (k_{decay}) vs the concentration of added quenchers:

$$k_{\text{decay}} = k_0 + k_q[Q] \quad (5)$$

O_2 and MMA quench this radical with bimolecular rate constants 1.1×10^9 and $2.9 \times 10^6 \text{ M}^{-1} \text{ s}^{-1}$, respectively.

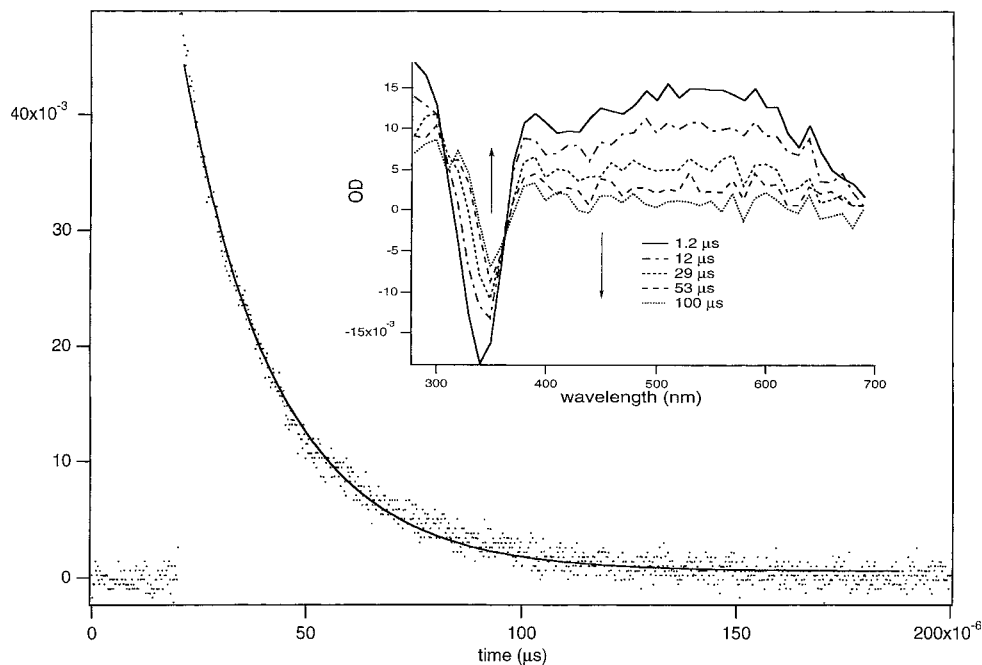


Figure 6. Time profile of transient absorption of **1** in benzene (1.02×10^{-4} M) monitored at 580 nm with fit residuals on the top. Inset: time-resolved transient absorption spectra of **1** in benzene at 355 nm excitation: after several decays (in μs).

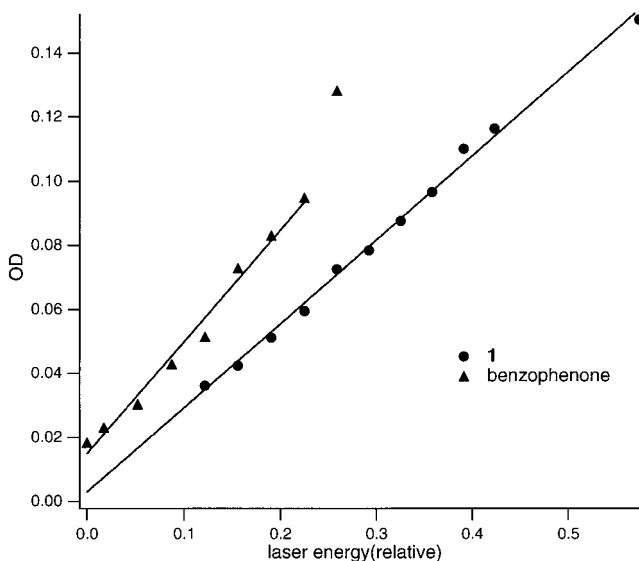


Figure 7. Dependence of the triplet-triplet absorption of **1** at 600 nm and benzophenone at 532 nm; optically matched deaerated benzene solutions ($\text{OD}_{355} = 0.5$), laser power; ($\epsilon_{\text{BP}}(532) = 8920 \text{ L mol}^{-1} \text{ cm}^{-1}$).

It was possible to determine the triplet quantum yield, ϕ_{T} , of **1** using the T-T extinction coefficient at 600 nm obtained from sensitized pulse radiolysis by laser excitation at 355 nm of optically matched benzene solutions ($\text{OD}_{355} = 0.5$) of **1** and of benzophenone (BP). BP is a known standard having a ϕ_{T} of unity^{31,32} (eq 6).³³ Plots of the intensities of the triplets of **1** and BP (Figure 7) as a function of the intensities of the triplets extrapolated to time zero gave slopes which, together with the known extinction coefficients, gave a ϕ_{T} for **1** of 0.97 ± 0.1 . This is clearly in agreement with the very low fluorescence quantum yield in this solvent.

$$\phi_{\text{T}}(\mathbf{1}) = \frac{\Delta\text{OD}_{\text{T}}(\mathbf{1})\epsilon_{\text{BP}}(532)}{\Delta\text{OD}_{\text{T}}(\text{BP})\epsilon_{\mathbf{1}}(600)}\phi_{\text{T}}(\text{BP}) \quad (6)$$

The results of the triplet quantum yield measurements and transient absorption spectra of **1** confirm the assumption that

the radicals come from the singlet excited state. The simultaneous growing in of radical absorption from the triplet state is not observed. Although the small $\text{S}_1\text{-T}_1$ splitting agrees with the presence of an n,π^* singlet, it may be that the triplet has a large degree of π,π^* character, possibly indicated by the long phosphorescence lifetime. This electronic configuration and the lower electronic energy relative to the corresponding phenyl derivatives may limit carbon-phosphorus bond cleavage.

In addition, a triplet quantum yield of almost unity may explain the inefficient formation of radicals since the formation of the triplet can be considered as an effective deactivation pathway of the singlet excited state that reduces the tendency for homolytic bond cleavage.

Surprisingly, laser flash photolysis of **1** in methanol after excitation at $\lambda_{\text{ex}} = 266 \text{ nm}$ gave a rather different transient absorption spectrum from those obtained in either benzene or acetonitrile (Figure 8).

Three transient signals were observed in methanol as (i) an absorption maximum at 330 nm, (ii) an emission maximum at 370 nm, and (iii) a further absorption maximum at 450 nm.

Second-order kinetics were observed for the 330 nm absorption (Table 2). This was assigned to the phosphinoyl radical using the known extinction coefficient³⁴ giving a rate constant for decay of $70.5 \text{ M}^{-1} \text{ s}^{-1}$. Bimolecular rate constants for quenching of the phosphinoyl radical by MMA and O_2 were 5.0×10^7 and $5.3 \times 10^8 \text{ M}^{-1} \text{ s}^{-1}$, respectively. These were obtained by eq 5 using a similar procedure to that used with the naphthoyl radical.

The absorption of the radical around 330 nm was not expected because, in aprotic solvents, we observed few radicals in the transient absorption spectra. As can be seen from Table 1, the intersystem crossing rate k_{isc} in methanol is slow ($\sim 10^8 \text{ s}^{-1}$) and fluorescence rate k_{f}^0 is fast ($\sim 10^7 \text{ s}^{-1}$) in comparison with that in other solvents ($\sim 10^9$ and 10^6 s^{-1}). As a result, in methanol k_{isc} and k_{f}^0 become competitive pathways. Since radical absorption rises at the same time as the absorption of the triplet states, the formation of the radical most likely occurs more often from the singlet excited state.

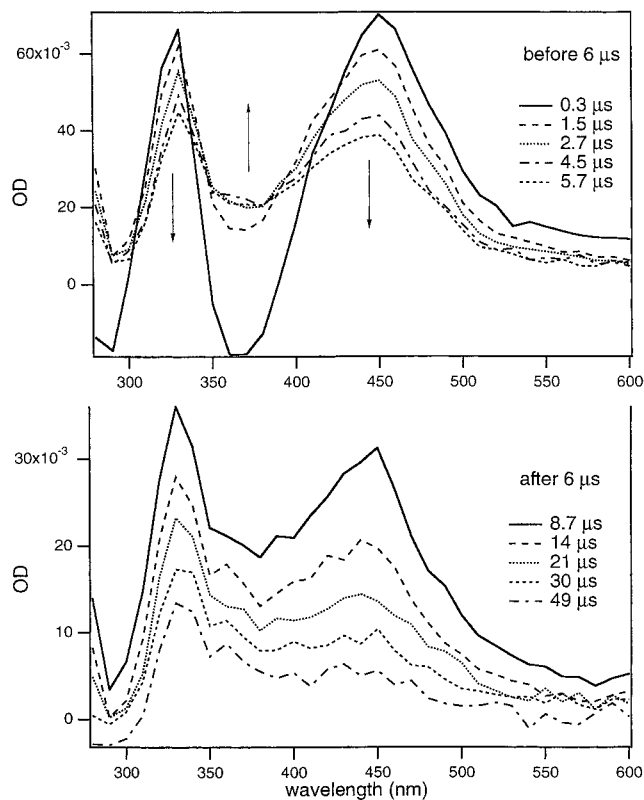


Figure 8. Time-resolved transient absorption spectra of **1** in methanol (9.29×10^{-5} M) at 266 nm excitation: after several decays (in μ s).

The transient absorption at 450 nm reveals monoexponential kinetics. Its rate of quenching by O_2 is on the order of one-ninth diffusion control quenching, indicating it to be the triplet. It has a similar decay to that observed in benzene and acetonitrile (Table 2). The transient species obtained at 370 nm is located in the same region as the steady state fluorescence in methanol and there is no ground state absorption in this region so this signal is assigned to fluorescence. After a few hundred nanoseconds, the emission is still observed in the transient absorption spectra. Before 6 μ s, this emission grows in; after 6 μ s, it disappears and decays at the same time as the triplet. We assign this transient as delayed fluorescence. Triplet-triplet annihilation produces the singlet excited state, which then gives this delayed fluorescence which is probably of the P-type. This is supported by time-resolved delayed fluorescence using the Spex and obtained after 1 μ s delay (Figure 1b). This emission falls in the same region as regular fluorescence. Its lifetime is calculated as 17 μ s after monoexponential fitting of the decay profile at 370 nm. This is less than the lifetime of triplet. This postulate is further confirmed by emission spectra obtained by nanosecond photolysis without analyzing light. The species decay monoexponentially with a lifetime 13.3 μ s, which is nearly half the triplet lifetime.

The kinetics at 370 nm show a fast growth of a transient absorption signal followed by a slow decay to a long-lived species. This absorption signal consists of complicated processes because of the overlap of several species including the phosphinoyl radical, the triplet, and the fluorescence emission. The slow decay kinetics at 370 nm was fitted to a decay time of 21 μ s. This has the similar decay time as the triplet at 450 nm.

Pulse Radiolysis in Benzene. Pulse radiolysis in benzene is an excellent technique for producing triplet excited states of solute molecules in high yield.³⁵ Thus, irradiation of a benzene

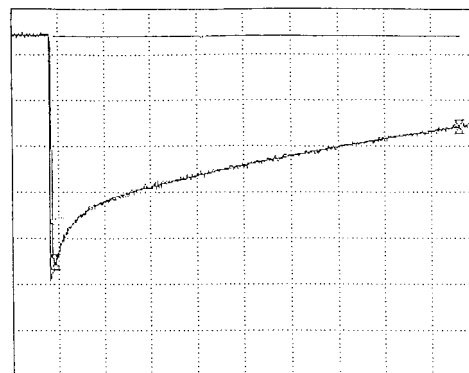
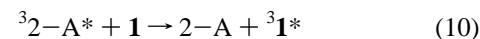
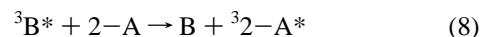
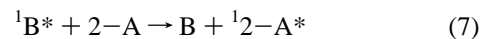


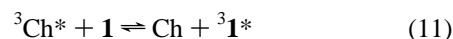
Figure 9. Transient absorption measured at 580 nm after irradiation of a deaerated benzene solution of Ch (9.8×10^{-3} mol L⁻¹) and **1** (2.2×10^{-4} mol L⁻¹) with a 20 ns electron pulse, 2 μ s/division, 2.0% absorption/division, $A_0 = 0.050$, $A_e = 0.035$ (0.029 corrected for absorption by $^3\mathbf{1}^*$).

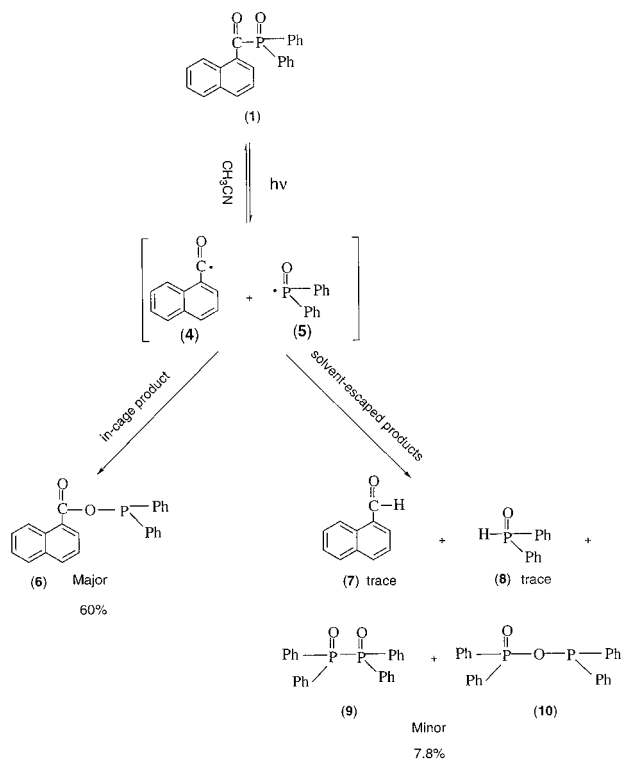
(B) solution of 2-acetonaphthone (2-A; 10^{-2} mol L⁻¹) containing **1** (10^{-4} mol L⁻¹) led to formation of a species with identical spectral characteristics to that observed by laser flash photolysis with $\lambda_{\text{max}} \sim 580\text{--}600$ nm. The species decayed cleanly with a first-order rate constant at low radiation dose ~ 55 μ s. This confirms the identity of the 580 nm species as the triplet state of **1**, produced here via the sequence of events summarized in eqs 7–10.³⁵ In addition, this experiment shows that the triplet energy of **1** is below that of 2-A (59.0 kcal mol⁻¹).



The extinction coefficient of the triplet state of **1** at 580 nm has been determined using the technique of Bensasson and Land.³¹ In these experiments two solutions of 2-A as above, one with and one without **1**, were subjected to pulse radiolysis. The $^32\text{-A}^*$ and $^3\mathbf{1}^*$ yields in terms of OD at their respective maxima, 430 and 580–600 nm, were obtained by extrapolating their decays back to time zero. The rate constant for energy transfer (cf. eq 10), determined to be 6.0×10^9 L mol⁻¹ s⁻¹ in a separate experiment, and the rate constant for natural decay of $^32\text{-A}^*$, 2.0×10^4 s⁻¹, showed that >98% of the latter were scavenged by **1**. The ratio of the extrapolated OD's and the known T–T extinction coefficient of 2-A ($10\,300$ L mol⁻¹ cm⁻¹)³¹ thus gave a value for **1** of 5000 L mol⁻¹ cm⁻¹ at 580 nm. Repetition using naphthalene (N), T–T extinction coefficient $13\,200$ L mol⁻¹ cm⁻¹ at 425 nm,³² instead of 2-A gave a value of 5360 L mol⁻¹ cm⁻¹, the average value being 5180 L mol⁻¹ cm⁻¹.

We have routinely determined triplet energies (E_T) in benzene by establishing equilibria for triplet energy transfer with a sensitizer of known E_T (cf. ref 35 and references therein). A particular advantage of this method is that large errors in K result in small errors in ΔG due to their exponential relationship. The two triplets need to be within ~ 4.0 kcal mol⁻¹ in energy for these experiments to work and the energy must be deposited initially within the highest energy sensitizer, i.e.; it must ideally have by far the higher concentration by a factor of 50 or more.³⁵ We have successfully established such an equilibrium between chrysene (Ch) and **1** (cf. eq 11 and Figure 9), the former clearly



SCHEME 1: Photochemistry of 1 (5×10^{-3} M) in Acetonitrile at 355 nm Irradiation

having the larger triplet energy. Thus, pulse radiolysis of a deaerated benzene solution of Ch ($E_T = 56.6 \text{ kcal mol}^{-1}$; $9.8 \times 10^{-3} \text{ mol L}^{-1}$) and **1** ($2.2 \times 10^{-4} \text{ mol L}^{-1}$) resulted in “immediate” formation of $^3\text{Ch}^*$, monitored at 580 nm. Since $^3\text{1}^*$ also absorbs at this wavelength but significantly less than chrysene ($29\,800\text{--}5180 \text{ L mol}^{-1} \text{ cm}^{-1}$) a simple correction could be made. The decay (Figure 9) was biexponential, showing fast decay to equilibrium followed by slow bleeding of that equilibrium. Extrapolation of the fast and slow decays to time zero gave optical densities corresponding to the concentrations of $^3\text{Ch}^*$ initially, A_0 , and at equilibrium, A_e (after correction). Because decay to equilibrium is fast relative to subsequent decay (cf. Figure 9), the equilibrium constant is given by $K = [\text{CH}]/[A_0 - A_e]/[1][A_e] = 22 \pm 5$, corresponding to $\Delta G = -1.8 \pm 0.2 \text{ kcal mol}^{-1}$. The standard assumption of no entropy change gives an E_T value for **1** of $54.8 \pm 0.1 \text{ kcal mol}^{-1}$. This is in excellent agreement with the value of $54.2 \text{ kcal mol}^{-1}$ obtained from phosphorescence data.

Steady State Photolysis and Product Analysis. Steady state irradiation of **1** in cyclohexane, benzene, or acetonitrile causes ground state bleaching and an isosbestic point in the UV spectra at 312 nm. Quantum yields for the disappearance of **1**, ϕ_d , determined by UV absorption spectroscopy using a standard solution 0.1 M benzophenone with 0.1 M benzhydrol in benzene with photoreduction quantum yield of 0.68,³⁶ possess considerably higher values in benzene (0.29) and acetonitrile (0.57). Photolysis of an aerated (0.005 M) acetonitrile solution of **1** gives the products shown in Scheme 1. Diphenyl[1-naphthoyl]oxy]phosphine (**6**)³⁷ is the major product. 1-Naphthaldehyde (**7**) and diphenylphosphine oxide (**8**) are minor products. Each was identified by comparison of NMR and GC/MS analysis with authentic samples. The structures of two isomeric diphosphorus photoproducts (**9**, **10**) have been tentatively assigned by ^{31}P NMR spectroscopy.¹²

The contradiction is that **1** has a highly efficient disappearance upon irradiation but yields no radicals that can be detected by laser flash photolysis. Since it also proves to be a poor photoinitiator,³⁸ this further implies that few radicals are generated. The efficient disappearance of **1** is attributed to the photoreaction of both singlet and triplet excited states. That is, the photoproducts may still arise from triplet excited state but do so by rearrangement in solvent cage. Major product **6** suggests the primary step may be carbon–phosphorus bond cleavage, but that subsequent recombination dominates in the solvent cage rather than cage escape. Thus, one recombination process gives both the starting material and product **6**. Such a recombination process commonly occurs with benzene derivatives **2** and **3**, although both the carbonyl radical and phosphinoyl radical can be detected by laser flash photolysis of UV and IR.

Conclusion

The photochemistry of **1** is dominated by a solvent cage process. Even though no radicals are detected except in methanol, the triplet has been detected by nanosecond laser flash photolysis as well as pulse radiolysis, and further characterized by triplet–triplet energy transfer. Hydrogen bonding has a dramatic effect on the fluorescence spectrum of **1** with a high fluorescence quantum yield being observed only in methanol. This is attributed to the elevation of the singlet excited state from n,π^* to π,π^* which then leads to a decreasing rate constant of intersystem crossing. The solvent indicator Reichardt’s dye gives the relative preferential solvation in methanol as being 13.4 times larger than that observed in acetonitrile, and suggests the dominant nature of methanol solvation. All of these facts clearly demonstrate that the extension of the chromophoric system alone in aryl–diphenylphosphine oxides is not sufficient in order to produce compounds with high quantum yields for α -cleavage.

Experimental Part

Materials and Solvents. (1-Naphthoyl)diphenylphosphine oxide was prepared according to a literature procedure³⁹ and recrystallized from cyclohexane before use.

Unless mentioned, all other chemicals and solvents (spectrophotometric grade) were obtained from Aldrich and used as received.

General Methods. Melting points were determined with a Thomas-Hoover capillary melting point apparatus and are uncorrected. NMR spectra were obtained either with a Varian Gemini 200 NMR spectrometer or Varian Unity Plus 400 NMR spectrometer. Chemical shifts are in ppm with TMS as the internal standard (^1H NMR and ^{13}C NMR) or H_3PO_4 as the external standard (^{31}P NMR). GC/MS and MS spectra were obtained on a Hewlett-Packard 5988 mass spectrometer coupled to an HP5880A GC, interfaced to an HP 2623A data processor. HPLC were taken by a Hewlett-Packard high-performance liquid chromatograph with a HP 1046A UV-absorbance detector. Quantitative HPLC analysis and separation was carried out on a RP-18 column and a mobile phase of a mixture of acetonitrile and water. Infrared spectra were taken with a Galaxy series 6020 FTIR spectrometer. Thin-layer chromatography was performed with Whatman silica gel coated TLC plates. Aldrich silica gel 60 Å (70–270 mesh) was used in column chromatography. Elemental analysis was performed by Atlanta Microlab, Inc.

Absorption spectra were recorded using a Hewlett-Packard 8452A diode array UV-vis spectrophotometer. Fluorescence and phosphorescence spectra were measured using a Spex Fluorolog 2 spectrophotometer. All spectra were measured using identical conditions of the instrument. Phosphorescence experiments were performed at 77 K in EPA (ether:isopentane:ethanol = 5:5:2) under argon. The source was a Xe lamp 3.0 ms pulse passed through monochromator. The quantum yields of fluorescence were determined relative to 9,10-diphenylanthracene.

(1-Naphthoyl)diphenylphosphine Oxide (1).³⁹ (55% yield): yellowish solid mp 157–158 °C; ¹H NMR (200 MHz, CDCl₃): δ 7.43–7.65 (m, 10 H), 7.86–7.92 (m, 3 H), 7.945 (d, *J* = 6.2 Hz, 1 H), 8.07 (d, *J* = 8.0 Hz, 1 H), 8.881 (d, *J* = 8.8 Hz, 1 H), 9.294 (d, *J* = 6.6 Hz); ¹³C NMR (50 MHz, CDCl₃): δ 124.749, 125.350, 126.788, 128.498, 128.753, 129.345 (d, *J* = 6.35 Hz), 130.136 (d, *J* = 7.31 Hz), 131.337, 131.865 (d, *J* = 9.1 Hz), 132.329 (d, *J* = 2.75 Hz), 133.293 (d, *J* = 50 Hz), 133.848, 135.886, 205.95 (d, *J* = 78.25 Hz); ³¹P NMR (CDCl₃): δ 23.532. MS: *m/e* 356(4), 327(0.12), 249-(0.14), 201(8.8), 183(1.5), 155(100), 127(60.7), 123(0.7); C₂₃H₁₇O₂P requires C: 77.52; H: 4.81 (found C: 77.26; H: 4.85).

Steady State Irradiation. (1-Naphthoyl)diphenylphosphine oxide was dissolved in acetonitrile in Pyrex test tubes, sealed with a rubber septum, bound by sticky Parafilm, and degassed by bubbling dry argon gas through the solution for 10–15 min. The solution was irradiated at 300–400 nm for 5 h in a Rayonet RPR 100 photoreactor, equipped with 16 350 nm F8T5-BLB UV lamps. Products were isolated by chromatography on silica gel with hexanes–ethyl acetate (4:1 to 1:6) as the eluent they were identified by comparison with authentic samples or characterized by spectral means.

Laser Flash Photolysis. Nanosecond laser flash photolysis experiments were carried out on a setup described by Ford and Rodgers using a Q-switched Nd:YAG laser as a pump light (355 nm; 60 mJ/pulse; 7 ns pulse or 266 nm; 5 mJ/pulse; 7 ns pulse).⁴⁰ Argon, oxygen, or air was bubbled continuously through the sample solution during the measurements.

Pulse Radiolysis. Single-wavelength experiments were obtained essentially as described with the exception that data were collected by means of a Tektronix TDS 754C digital storage oscilloscope. Analytical routines being performed on a DAN 486 PC using in-house software.⁴¹

The multiwavelength system was essentially as described, but with the prototype acrylic lens rod and optical fibers replaced by quartz equivalents. Analytical software was written in-house and routines performed on a DAN 486 PC.⁴²

Acknowledgment. We thank the National Science Foundation, Division of Materials Research (NSF 9526755), and the Office of Naval Research Polymers Program (N00014-97-1-0834) for financial support of this work. Conversations with Prof. G. S. Hammond and Prof. M. A. J. Rodgers are gratefully acknowledged. The authors also gratefully acknowledge the use of transient facilities from the laboratories of Professor M. A. J. Rodgers. Pulse radiolysis experiments were performed at the Paterson Institute for Cancer Research Free Radical Research Facility, the Christie Hospital NHS Trust, Manchester. The Facility is funded under the European Commission TMR PROGRAMME—ACCESS TO LARGE SCALE FACILITIES, Grant ERBFMGECT 950084. A research fellowship granted

by the McMaster Endowment to N. Zhao is also gratefully acknowledged.

References and Notes

- (1) Contribution 383 from the Center for Photochemical Sciences.
- (2) Jacobi, M.; Henne, A. *J. Radiat. Curing* **1983**, *10*, 16.
- (3) Jacobi, M.; Henne, A. *Polym. Paint Color J.* **1985**, *175*, 636.
- (4) Oldering, P. K. T. *Chemistry and Technology of UV and EB Formulation for Coatings, Inks and Paints*; SITA Technology Ltd.: London, 1991; Vol. 3, 168.
- (5) Sumiyoshi, T.; Schnabel, W.; Henne, A.; Lechtken, P. *Polymer* **1985**, *26*, 141.
- (6) Sumiyoshi, T.; Schnabel, W. *Makromol. Chem.* **1985**, *186*, 1811.
- (7) Majima, T.; Schnabel, W. *J. Photochem. Photobiol. A: Chem.* **1991**, *58*, 239.
- (8) Sumiyoshi, T.; Schnabel, W.; Henne, A. *J. Photochem.* **1986**, *32*, 119.
- (9) Sumiyoshi, T.; Schnabel, W.; Henne, A. *J. Photochem.* **1986**, *32*, 191.
- (10) Sumiyoshi, T.; Schnabel, W.; Henne, A. *J. Photochem.* **1985**, *30*, 63.
- (11) (a) Roberts, B. P.; Singh, K. J. *J. Organomet. Chem.* **1978**, *159*, 31. (b) Kamachi, M.; Kuwata, K.; Sumiyoshi, T.; Schnabel, W. *J. Chem. Soc., Perkin Trans. 2*, **1988**, 961. (c) Turro, N. J.; Khudyakov, I. V. *Chem. Phys. Lett.* **1992**, *193*, 546. (d) Kajiwara, A.; Konishi, Y.; Schnabel, W.; Kuwata, K.; Kamachi, M. *Macromolecules* **1993**, *26*, 1656. (e) Kamachi, M.; Kajiwara, A.; Saegusa, K.; Morishiwa, Y. *Macromolecules* **1993**, *26*, 7369.
- (12) Kolezak, U.; Rist, G.; Dietliker, K.; Wirz, J. *J. Am. Chem. Soc.* **1996**, *118*, 6477.
- (13) Sluggett, G. W.; Turro, C.; George, M. W.; Koptuyg, I. V.; Turro, N. J. *J. Am. Chem. Soc.* **1995**, *117*, 5148.
- (14) Sluggett, G. W.; McGarry, P. F.; George, M. W.; Koptuyg, I. V.; Turro, N. J. *J. Am. Chem. Soc.* **1996**, *118*, 7367.
- (15) Jockusch, S.; Koptuyg, I. V.; McGarry, P. F.; Sluggett, G. W.; Turro, N. J.; Watkins, D. M. *J. Am. Chem. Soc.* **1997**, *119*, 11495.
- (16) (a) Baxter, J. E.; Davison, R. S. *Macromol. Chem. Rapid Commun.* **1987**, *8*, 311. (b) Baxter, J. E.; Davison, R. S. *Macromol. Chem.* **1988**, *189*, 2769.
- (17) Beechem, J. M.; Gratton, E.; Amelot, M.; Knutson, J. R.; Brand, L. In *Topics in Advanced Fluorescence Spectroscopy*; Lakowicz, J. R., Ed.; Plenum Press: New York, 1991; Vol. 2, p 241.
- (18) Turro, N. J., Ed., *Modern Molecular Photochemistry*; The Benjamin/Cummings Publishing: Menlo Park, CA, 1978.
- (19) The origin of eq 1 belongs to the Strickler–Berg treatment. We used eq 1 to discuss differences in our experiments, and this showed that the k_f^0 data obtained in aprotic solvents are approximately of the same order. Data are not available for methanol because the molecule is insufficiently solvated. The original reference can be found in: Strickler, S. J.; Berg, R. J. *J. Chem. Phys.* **1962**, *37*, 814.
- (20) El-Sayed, M. A. *J. Chem. Phys.* **1963**, *38*, 2834.
- (21) Kitamura, M.; Baba, H. *Bull. Chem. Soc. Jpn.* **1975**, *48*, 1191.
- (22) Murov, S. L.; Carmichael, I.; Hug, G. L. *Handbook of Photochemistry*, 2nd ed.; Marcel Dekker: New York, 1993.
- (23) Sanyo, H.; Hirayama, F. *J. Phys. Chem.* **1983**, *87*, 83.
- (24) Scaiano, J. C., Ed. *Handbook of Organic Photochemistry*; CRC Press: Boca Raton, FL, 1989; Vol. 1, p 237.
- (25) Bradley, G. J.; Kasha, M. *J. Am. Chem. Soc.* **1955**, *77*, 4462.
- (26) Reichardt, C. *Chem. Rev.* **1994**, *94*, 2319.
- (27) Bosch, E.; Roses, M. *J. Chem. Soc., Faraday Trans.* **1992**, *88*, 3541.
- (28) (a) Marquardt, D. W. *Soc. Ind. Appl. Math.* **1963**, *11*, 431. (b) Levenberg, K. *Q. Appl. Math.* **1944**, *2*, 164.
- (29) The program IGOR Pro 3.11 from Wavemetrics Inc. was used for global analysis.
- (30) According to the second-order kinetic law where $1/c = (1/c_0) + kt$, our data were transformed such that they can be plotted according to this treatment. It is easier to distinguish if the data belong to a second-order kinetic law or not because this is a linear function.
- (31) Gorman, A. A.; Hamblett, I.; Lambert, C.; Prescott, A. L.; Rodgers, M. A. J.; Spence, H. M. *J. Am. Chem. Soc.* **1987**, *109*, 3091.
- (32) Bensasson, R. V.; Land, E. *J. Photochem. Photobiol. Rev.* **1978**, *3*, 163.
- (33) Carmichael, I.; Hug, G. L. *J. Phys. Chem. Ref. Data* **1986**, *15*(1), 1.

- (34) Sumiyoshi, T.; Schnabel, W. *J. Photochem.* **1986**, 32, 119.
- (35) Gorman, A. A.; Hamblett, I.; Irvine, M.; Raby, P.; Standen, M. C.; Yeates, S. *J. Am. Chem. Soc.* **1985**, 107, 4404
- (36) Moore, W. M.; Ketchum, M. *J. Am. Chem. Soc.* **1962**, 84, 1368.
- (37) Brierley, J.; Dickstein, J. I.; Trippett, S. *Phosphorus, Sulfur Relat. Elem.* **1979**, 7, 167.
- (38) Hu, S.; Popielarz, R.; Neckers, D. C. *Macromolecules* **1998**, 31, 4107.
- (39) (a) Ger. Offen. 2830927 (1980), BASF AG.; invs.: Lechtken, P.; Buehe, I.; Hesse, A. (b) Berlin, K. D.; Taylor, H. A. *J. Am. Chem. Soc.* **1964**, 86, 3826.
- (40) Ford, W. E.; Rodgers, M. A. J. *J. Phys. Chem.* **1994**, 98, 3822.
- (41) Gorman, A. A.; Hamblett, I. *Chem. Phys. Lett.* **1983**, 97, 422.
- (42) Lubis, R.; Allan, D.; Hodgson, B. W.; Swallow, A. J. *Radiat. Phys. Chem.* **1992**, 39, 7.